

Electroweak gauge boson production at $\gamma\gamma$ collider *

G. Jikia[†]

*Albert-Ludwigs-Universität Freiburg, Fakultät für Physik
Hermann-Herder Str.3, D-79104 Freiburg, Germany*

and

*Institute for High Energy Physics, Protvino
Moscow Region 142284, Russian Federation*

1. Introduction

Linear colliders offer unique opportunities to study high energy photon-photon collisions obtained using the process of Compton backscattering of laser light off electron beams from the linear collider [1]. This option is included now in conceptual design reports of the NLC, JLC and TESLA/SBLC projects of e^+e^- linear collider [2,3]. The expected physics at the Photon Linear Collider (PLC) is very rich and complementary to that in e^+e^- collisions. In particular PLC will be especially attractive tool in probing the the electroweak symmetry breaking sector via precision measurements of anomalous W self couplings. In this paper a short survey of the most important processes of electroweak gauge boson production in photon-photon collisions is given.

2. $\gamma\gamma \rightarrow W^+W^-$ cross sections and quantum $\mathcal{O}(\alpha)$ corrections

The reaction $\gamma\gamma \rightarrow W^+W^-$ would be the dominant source of the W^+W^- pairs at future linear colliders, provided that photon-photon collider option will be realized. The Born cross section of W^+W^- pair production in photon-photon collisions in the scattering angle interval $10^\circ < \theta^\pm < 170^\circ$ is 61 pb at $\sqrt{s_{\gamma\gamma}} = 500$ GeV and 37 pb at 1 TeV. Corresponding cross sections of W^+W^- pair production in e^+e^- collisions are an order of magnitude smaller: 6.6 pb at 500 GeV and 2.5 pb at 1 TeV. With more than a million WW pairs per year a photon-photon collider can be really considered as a W -factory and an ideal place to conduct precision tests on the anomalous triple and quartic couplings of the W bosons.

With the natural order of magnitude on anomalous couplings one needs to know the \mathcal{SM} cross sections with a precision better than 1% to extract these small numbers. From a theoretical point of view this calls for the very careful analysis of at least $\mathcal{O}(\alpha)$ corrections to the cross section of W^+W^- pair production in $\gamma\gamma$ collisions, which were recently calculated including virtual corrections [4] and including complete $\mathcal{O}(\alpha)$ corrections with account of both virtual one-loop corrections and real photon and Z -boson emission [5].

Figure 1 shows total cross section of WW pair production summed over WW and $WW\gamma$ final states and integrated over W^\pm scattering angles in the interval $10^\circ < \theta^\pm < 170^\circ$ as a function of

*Talk presented at the *International Workshop on Linac-Ring Type ep and γp Colliders*, 9–11 April 1997, Ankara, Turkey

[†]Alexander von Humboldt Fellow; e-mail: jikia@phyv4.physik.uni-freiburg.de

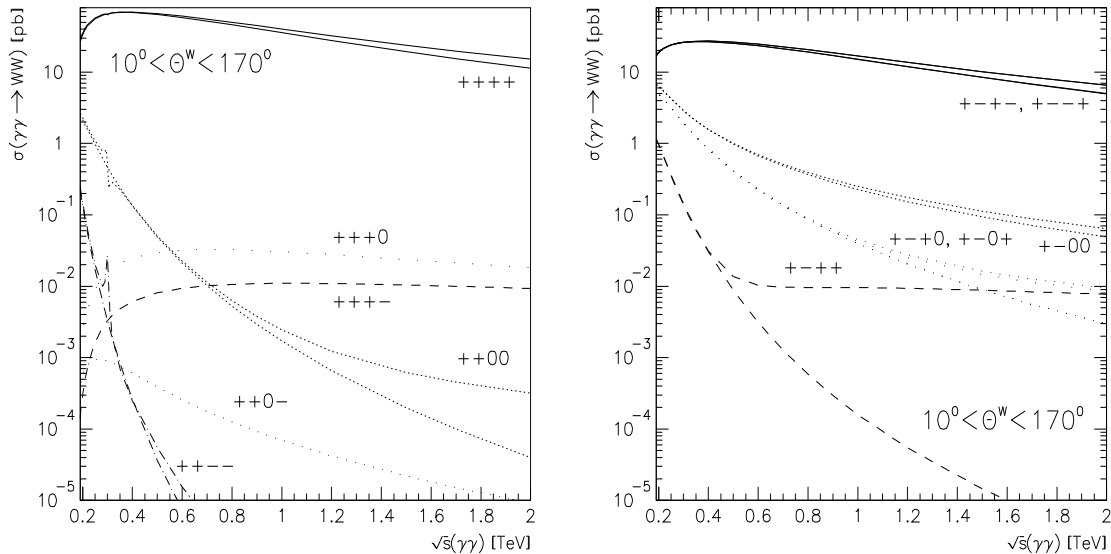


Fig. 1. Total cross sections of $WW(\gamma)$ production for various polarizations. Born and corrected cross sections are shown. The curves nearest to the helicity notations represent the corrected cross sections.

energy for various polarizations [5]. The bulk of the cross section originates from transverse $W_T W_T$ pair production. Transverse W 's are produced predominantly in the forward/backward direction and the helicity conserving amplitudes are dominating. Cross sections integrated over the whole phase space are non-decreasing with energy. For a finite angular cutoff they do decrease as $1/s$, but still they are much larger than suppressed cross sections. For the dominating $++ ++$, $+ - + -$, $+ - - +$ helicity configurations corrections are negative and they rise with energy ranging from -3% at 500 GeV to -25% at 2 TeV.

In Table 1 Born cross sections and relative corrections are given for several intervals of W^\pm scattering angles [5]. At high energies large cancellations occur between negative virtual corrections and positive corrections corresponding to real photon or Z -boson emission. Consequently, although the correction originating from the WWZ production is completely negligible at $\sqrt{s_{\gamma\gamma}} = 0.3$ TeV, it is of the same order of magnitude as hard photon correction at 2 TeV. Although at 300 \div 500 GeV corrections are quite small ranging from -1.3% to -8% , depending on angular cuts, at TeV energies the value of radiative corrections in the central region of W^+W^- production become quite large, so that corrections in the region $60^\circ < \theta < 120^\circ$ are 6 \div 8 times larger than the corrections to the total cross section at 1 \div 2 TeV. They range from -24% to -45% . Thus if precision measurements are to be made at TeV energy, more careful theoretical analysis could be needed in order to reliably predict the value of the cross section in the central region where the value of the cross section is the most sensitive to the W anomalous couplings.

Table 1. Total unpolarized Born cross sections and relative corrections for various intervals of W^\pm scattering angles. Corrections originating from real hard photon ($\omega_\gamma > k_c = 0.1$ GeV) and Z -boson emission as well as IR-finite sum of soft photon and virtual boson contributions, fermion virtual corrections and total corrections are given separately.

$$\sqrt{s} = 300 \text{ GeV}$$

$\theta_{W^\pm}, ^\circ$	σ^{Born}, pb	$\delta^{hard}, \%$	$\delta^Z, \%$	$\delta^{soft+bose}, \%$	$\delta^{fermi}, \%$	$\delta^{tot}, \%$
$0^\circ < \theta < 180^\circ$	70.22	4.15	$2.64 \cdot 10^{-2}$	-7.09	0.327	-1.37
$10^\circ < \theta < 170^\circ$	64.46	4.11	$2.74 \cdot 10^{-2}$	-7.31	0.257	-1.59
$30^\circ < \theta < 150^\circ$	38.15	4.09	$3.27 \cdot 10^{-2}$	-8.62	-0.123	-2.67
$60^\circ < \theta < 120^\circ$	12.96	4.02	$2.94 \cdot 10^{-2}$	-10.7	-0.415	-3.75

$$\sqrt{s} = 500 \text{ GeV}$$

$\theta_{W^\pm}, ^\circ$	σ^{Born}, pb	$\delta^{hard}, \%$	$\delta^Z, \%$	$\delta^{soft+bose}, \%$	$\delta^{fermi}, \%$	$\delta^{tot}, \%$
$0^\circ < \theta < 180^\circ$	77.50	7.96	0.468	-10.1	$9.04 \cdot 10^{-2}$	-1.63
$10^\circ < \theta < 170^\circ$	60.71	7.89	0.541	-10.7	-0.242	-2.52
$30^\circ < \theta < 150^\circ$	21.85	8.05	0.817	-13.0	-1.34	-5.50
$60^\circ < \theta < 120^\circ$	5.681	8.02	0.789	-14.8	-2.13	-8.12

$$\sqrt{s} = 1000 \text{ GeV}$$

$\theta_{W^\pm}, ^\circ$	σ^{Born}, pb	$\delta^{hard}, \%$	$\delta^Z, \%$	$\delta^{soft+bose}, \%$	$\delta^{fermi}, \%$	$\delta^{tot}, \%$
$0^\circ < \theta < 180^\circ$	79.99	13.3	1.55	-18.7	$-5.51 \cdot 10^{-2}$	-3.89
$10^\circ < \theta < 170^\circ$	37.04	13.4	2.39	-22.6	-1.28	-8.10
$30^\circ < \theta < 150^\circ$	6.924	14.2	3.96	-32.1	-3.80	-17.8
$60^\circ < \theta < 120^\circ$	1.542	14.2	3.88	-37.1	-5.13	-24.1

$$\sqrt{s} = 2000 \text{ GeV}$$

$\theta_{W^\pm}, ^\circ$	σ^{Born}, pb	$\delta^{hard}, \%$	$\delta^Z, \%$	$\delta^{soft+bose}, \%$	$\delta^{fermi}, \%$	$\delta^{tot}, \%$
$0^\circ < \theta < 180^\circ$	80.53	19.0	2.91	-27.2	$-7.45 \cdot 10^{-2}$	-5.33
$10^\circ < \theta < 170^\circ$	14.14	20.1	6.38	-41.6	-2.99	-18.1
$30^\circ < \theta < 150^\circ$	1.848	21.5	9.77	-60.1	-6.54	-35.4
$60^\circ < \theta < 120^\circ$	0.3936	21.6	9.60	-67.6	-8.04	-44.5

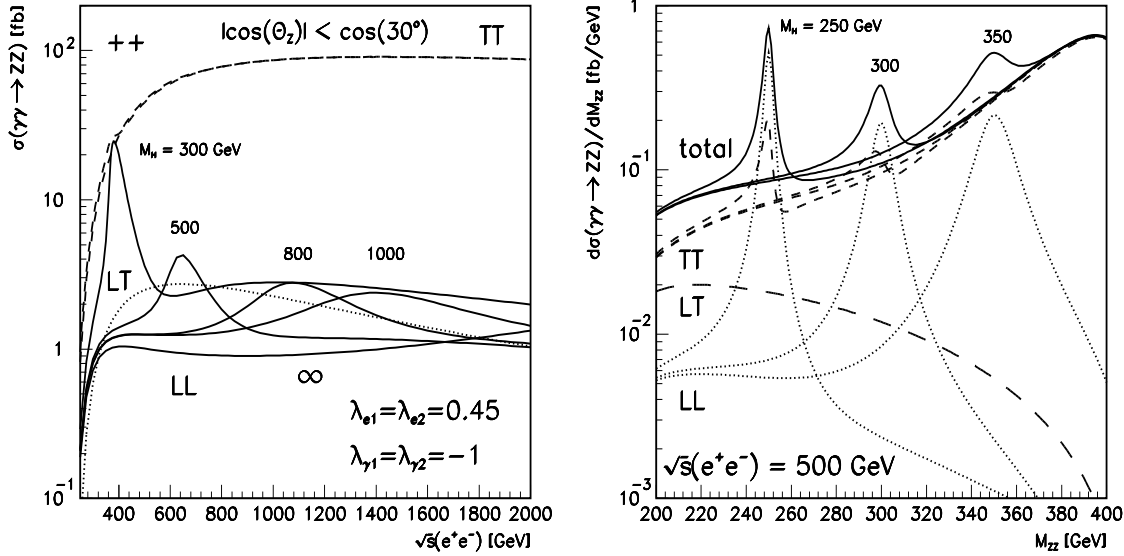


Fig. 2. (a) Cross section of the ZZ pair production in polarized $\gamma\gamma$ collisions versus c.m.s. energy of the e^+e^- collisions computed taking into account photon spectrum of the backscattered laser beams. Both Z -bosons have $|\cos\theta_Z| < \cos 30^\circ$. Curves for $Z_L Z_L$ (solid line), $Z_T Z_T$ (dashed line) and $Z_L Z_T$ (dotted line) production are shown. Different curves for longitudinal $Z_L Z_L$ pair production correspond to Higgs boson masses of 300, 500, 800, 1000 GeV and infinity. (b) The invariant mass, M_{ZZ} , distribution of Z -bosons for $\gamma\gamma \rightarrow ZZ$ in photon-photon collisions at $\sqrt{s_{e^+e^-}} = 500$ GeV and $m_H = 250, 300$ and 350 GeV. Curves for $Z_L Z_L$ (dotted line), $Z_T Z_T$ (dashed line) and $Z_L Z_T$ (long dashed line) production are shown in addition to the sum over all polarizations of the Z -boson (solid line).

3. $\gamma\gamma \rightarrow ZZ$ production

Z -pair production in photon-photon collisions plays a special role due to the possibility to observe the Higgs signal in $\gamma\gamma$ collisions for the Higgs bosons heavier than $2M_Z$ in ZZ decay mode [6, 7] if one of the Z 's is required to decay to l^+l^- to suppress the huge tree-level $\gamma\gamma \rightarrow W^+W^-$ continuum background. However, even though there is no tree-level ZZ continuum background, such a background due to the reaction $\gamma\gamma \rightarrow ZZ$ does arise at the one-loop level in the electroweak theory [8–11] which makes the Higgs observation in the ZZ mode impossible for $m_h \gtrsim (350 \div 400)$ GeV. It was found that for $185 \lesssim m_h \lesssim 300$ GeV the ZZ mode will provide a 10-20% determination of the quantity $\Gamma(h \rightarrow \gamma\gamma) \cdot BR(h \rightarrow ZZ)$.

In Fig. 2 the cross section of the ZZ pair production and invariant mass distribution at the PLC are shown [8]. With the polarizations of the initial electron (positron) and laser beams shown, the photon-photon energy spectrum peaks just below the highest allowed photon-photon energy and colliding photons are produced mainly with equal mean helicities $\langle \xi_1 \xi_2 \rangle \sim 1$. As for the case of W pair production, at high energies the cross section is dominated by the transversely polarized $Z_T Z_T$ pair production. As it was already mentioned, while clear Higgs boson peaks are observable at $\sqrt{s_{e^+e^-}} = 500$ GeV for $m_H = 250$ and 300 GeV in Fig. 2b, a background from transverse $Z_T Z_T$

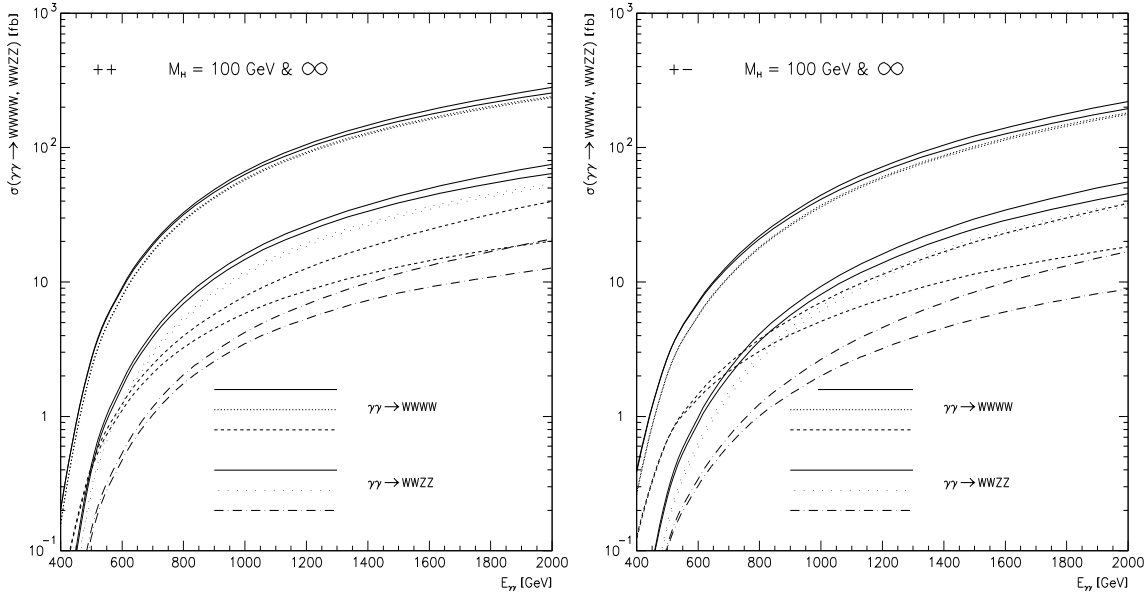


Fig. 3. Comparison between the cross sections for $m_H = 100$ GeV and $m_H = \infty$ for equal and opposite helicities of the initial photons. For the reaction $\gamma\gamma \rightarrow WWWW$ the following cross sections are shown: total cross section (solid line), the $TTTT + TTTL$ cross sections (dotted line), the sum of cross sections with at least two longitudinal final W 's (dashed line). For the reaction $\gamma\gamma \rightarrow WWZZ$ corresponding cross sections are denoted by solid, dotted and dash-dotted lines.

pair production makes the observation of heavier Higgs signal quite problematic.

4. $W^+W^- \rightarrow W^+W^-, ZZ$ scattering

At center-of-mass energy above 1 TeV the effective W luminosity becomes substantial enough to allow for the study of $W^+W^- \rightarrow W^+W^-$, ZZ scattering in the reactions $\gamma\gamma \rightarrow WWWW$, $WWZZ$, when each incoming photon turns into a virtual WW pair, followed by the scattering of one W from each such pair to form WW or ZZ .

It was found [12, 13] that a signal of SM Higgs boson with m_h up to 700 GeV (1 TeV) could be probed in these processes at 1.5 TeV (2 TeV) PLC, assuming integrated luminosity of 200 fb^{-1} (300 fb^{-1}). However even larger luminosity is needed in order to extract the signal of enhanced $W_L W_L$ production in models of electroweak symmetry breaking without Higgs boson [12]. The main problem is again large background from transverse $W_T W_T W_T W_T$, $W_T W_T Z_T Z_T$ production.

Event rates as well as signal/background ratio and the statistical significance corresponding to various values of the Higgs boson mass and cosine of the dead cone angle z_0 are given in Table 2 for total energies of 1.5 and 2 TeV [12]. The value of integrated luminosity of 200 fb^{-1} is assumed and branching ratio of 50% for hadronic decays of WW , ZZ pairs is included. At $\sqrt{s} = 1.5$ TeV we require that the invariant mass M_{34} of central pair WW , ZZ lie in the interval $400 \text{ GeV} < M_{34} < 600 \text{ GeV}$ for $m_H = 500$ GeV and $500 \text{ GeV} < M_{34} < 800 \text{ GeV}$ for $m_H = 700$ GeV. For $m_H = 1$ TeV and $\sqrt{s} = 2$ TeV $450 \text{ GeV} < M_{34} < 1.1$ TeV.

As one can see from Fig. 3 the contribution from two longitudinal weak bosons $TTLL$ and

Table 2. Event rates for signal (S) and background (B) summed over $WWWW$ and $WWZZ$ final states as well as signal/background ratio and statistical significance.

		$z_0 = \cos(10^\circ)$				$z_0 = \cos(5^\circ)$			
$\sqrt{s_{e^+e^-}}$, TeV	m_H , GeV	S	B	S/B	S/\sqrt{B}	S	B	S/B	S/\sqrt{B}
1.5	500	84	34	2.5	14	218	56	3.9	29
	700	24	23	1.0	5.0	53	37	1.4	8.7
2	1000	14	21	0.67	3.0	74	59	1.3	9.6

$TLTL$, which are sensitive to heavy Higgs boson contribution, are about an order of magnitude smaller than that for $TTTT$ production [12]. So, for the total cross sections one should expect 10% signal-to-background ratio.

5. $\gamma\gamma \rightarrow \gamma\gamma, \gamma Z$

Neutral gauge boson $\gamma\gamma, \gamma Z, ZZ$ pair production processes in photon-photon fusion represent special interest because these processes are absent at the classical level and are generated at the one-loop level due to quantum corrections. The collision of high energy, high intensity photon beams at the Photon Collider would provide novel opportunities for such processes. The distinctive feature of the electroweak vector boson loops contribution is that it leads to the differential cross sections behaving as $d\sigma/dt \propto 1/t^2$ in the high energy limit and, hence, to a nondecreasing with energy total cross sections.

The total cross sections of $\gamma\gamma, \gamma Z$ pair production are shown in Figs. 4, 5, respectively. W loop contribution dominates at photon-photon collision energies above 250 GeV.

In fact, the measurement of $\gamma\gamma \rightarrow \gamma Z$ cross section is a measurement of $Z\gamma\gamma\gamma$ coupling, which could be also measured in three photon Z decay. However, it is well known, decay of the Z boson into three photons via both fermion and W boson loops in SM has too small branching ratio (of the order of $3 \cdot 10^{-10}$ [16]) to be observed at LEP experiments. From the other side, at PLC the γZ final state, which should be background free, has the largest observable rate (if no light Higgs boson is present) in comparison to $\gamma\gamma$ and ZZ (*e.g.*, a three hundred γZ pairs yearly can be produced at the Photon Collider realized at the 500 GeV electron linear collider). So, even the unique Standard Model $\gamma\gamma\gamma Z$ vertex can be measured in photon-photon collisions. Numerical values of the total cross section (with the angular cuts imposed) are given in Table 3 [15].

Table 3. Event rates for γZ pair production at PLC

$\sqrt{s_{e^+e^-}}$	300 GeV	500 GeV	1 TeV
$\sigma(\gamma\gamma \rightarrow \gamma Z_T)$	9.3 fb	32 fb	53 fb
$\sigma(\gamma\gamma \rightarrow \gamma Z_L)$	0.28 fb	0.51 fb	0.39 fb

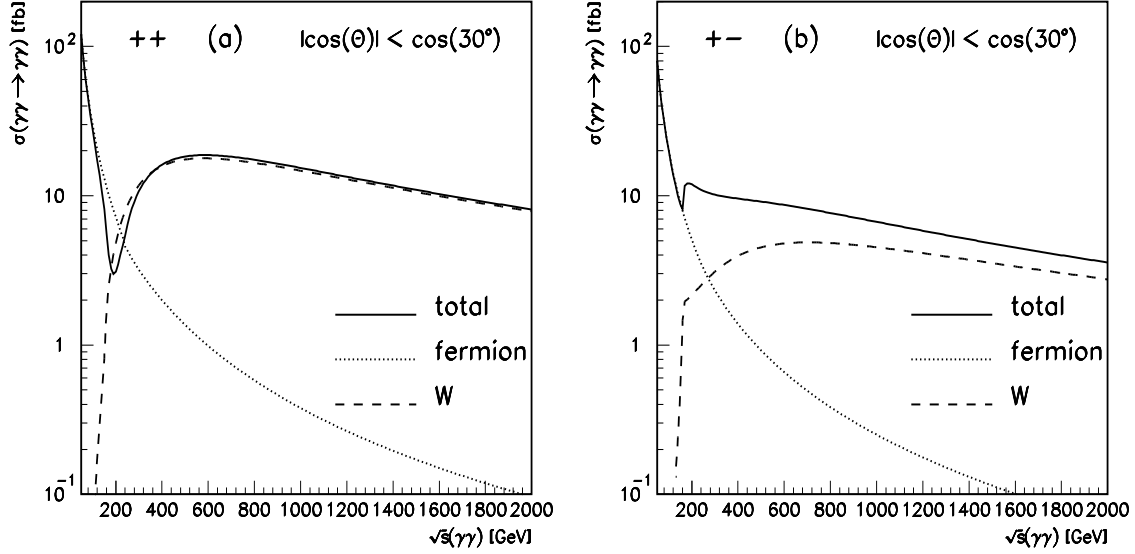


Fig. 4. Total cross section of photon-photon scattering in monochromatic photon-photon collisions versus $\gamma\gamma$ c.m. energy for different helicities of the incoming photons. Total cross section (solid line) as well as W boson loop contribution (dashed line) and fermion loop contribution (dotted line) are shown.

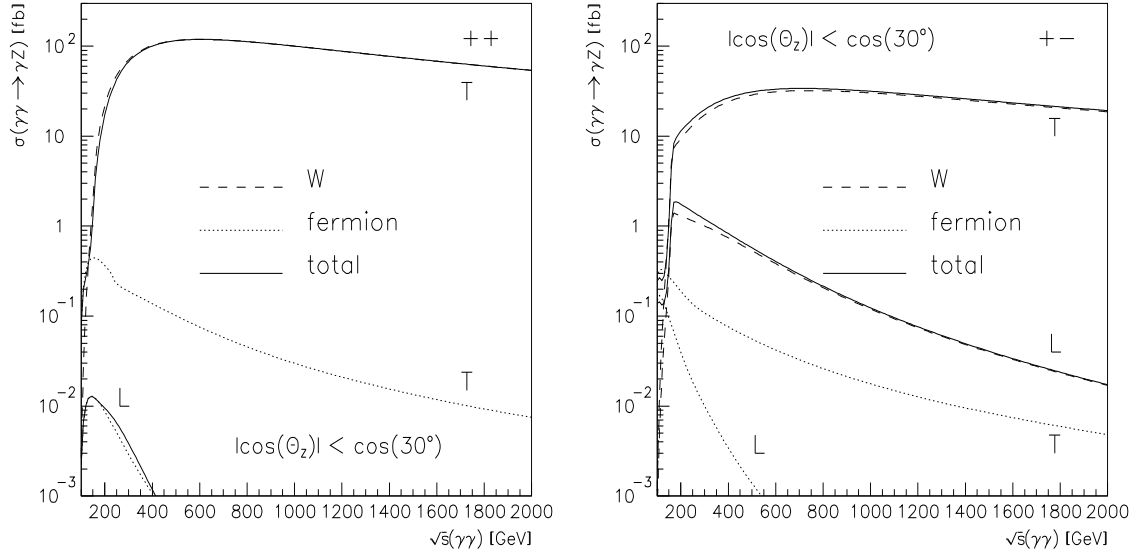


Fig. 5. Total cross section of γZ pair production in monochromatic photon-photon collisions versus $\gamma\gamma$ c.m. energy for different helicities of the incoming photons and final Z boson. Total cross section (solid line) as well as W boson loop contribution (dashed line) and fermion loop contribution (dotted line) are shown.

References

- [1] V. Telnov, These Proceedings and references therein.
- [2] NLC ZDR Design Group and NLC Physics Working Group (S. Kuhlman et al.), SLAC-R-0485, June 1996, hep-ex/9605011.
- [3] R. Brinkmann *et al.*, DESY-79-048, July 1997, hep-ex/9707017.
- [4] A. Denner, S. Dittmaier, and R. Schuster, *Nucl. Phys.* **B452** (1995) 80; Proceedings of the 3rd Workshop e^+e^- Collisions at TeV Energies: the Physics Potential, Part D, DESY, Hamburg, Germany, August 30 – September 1, 1995, p. 233; Report BI-TP 96/03, WUE-ITP-96-001, hep-ph/9601355.
- [5] G. Jikia, Proceedings of the Workshop Physics and Experiments with Linear e^+e^- Colliders, Morioka, Japan, September 8–12, 1995; *Nucl. Phys.* **B494** (1997) 19.
- [6] D. Borden, D. Bauer, D.O. Caldwell, *SLAC-PUB-5715*, *UCSD-HEP-92-01*; *Phys. Rev.* **D48** (1993) 4018.
- [7] J.F. Gunion and H.E. Haber, *Phys. Rev.* **D48** (1993) 5109.
- [8] G. Jikia, *Phys. Lett.* **B298** (1993) 224; *Proc. of the 2nd Workshop on “Physics and Experiments with Linear e^+e^- Colliders”*, eds. F. Harris, S. Olsen, S. Pakvasa and X. Tata, Waikoloa (1993) World Scientific Publishing, Singapore, p. 558; *Nucl. Phys.* **B405** (1993) 24.
- [9] M.S. Berger *Phys. Rev.* **D48** (1993) 5121.
- [10] D.A. Dicus and C. Kao, *Phys. Rev.* **D49** (1994) 1265.
- [11] H. Veltman, *Z. Phys.* **C62** (1994) 235.
- [12] G. Jikia, Proc. of the *Workshop on gamma–gamma colliders*, March 28-31, 1994, Lawrence Berkeley Laboratory, *Nucl. Instr. & Meth.* **A355** (1995) 84; *Nucl. Phys.* **B437** (1995) 520.
- [13] K. Cheung, *Phys. Lett.* **B323** (1994) 85; *Phys. Rev.* **D50** (1994) 4290.
- [14] G. Jikia, A. Tkabladze, *Phys. Lett.* **B323** (1994) 453.
- [15] G. Jikia, A. Tkabladze, *Phys. Lett.* **B332** (1994) 441.
- [16] M. Baillargeon and F. Boudjema, *Phys. Lett.* **B272** (1991) 158; F.X. Dong, X.D. Jiang and X.J. Zhou, *Phys. Rev.* **D46** 1992 5074; E.W.N. Glover and A.G. Morgan, *Z. Phys.* **C60** 1993 175.